Chronic obesity does not alter cancer survival in *Tp53*$^{R270H/+}$ mice

Ilaria Panzeri[1,2], Zachary Madaj[3], Luca Fagnocchi[1], Stefanos Apostle[1], Megan Tompkins[4], Galen Hostetter[5], J. Andrew Pospisilik[1,2,*]

[1] Department of Epigenetics, Van Andel Institute, Grand Rapids, MI, USA
[2] Department of Epigenetics, Max Planck Institute of Immunobiology and Epigenetics, Freiburg, Germany
[3] Bioinformatics and Biostatistics Core, Van Andel Institute, Grand Rapids, MI, USA
[4] Vivarium and Transgenics Core, Van Andel Institute, Grand Rapids, MI, USA
[5] Pathology and Biorepository Core, Van Andel Institute, Grand Rapids, MI, USA

[*]Correspondence: andrew.pospisilik@vai.org

Abstract

Obesity is a complex chronic disease characterized by excessive adiposity and associations with numerous co-morbidities, including cancer. Despite extensive research, we have limited understanding of the mechanisms coupling obesity to cancer risk, and, of the contexts in which obesity does or does not exacerbate disease. Here, we show that chronic high-fat diet (HFD)-induced obesity has no significant effect on the *Tp53*$^{R270H/+}$ mouse, a model of human Li-Fraumeni multi-cancer syndrome. Surprisingly, despite inducing rapid and highly penetrant obesity and long-term differences in metabolic and adiposity, greater than one year of HFD had no significant effect on survival or tumor burden. These findings were replicated in two separate cohorts and thus provide important negative data for the field. Given strong publication bias against negative data in the literature, this large cohort study represents a clear case where chronic diet-induced obesity does not accelerate or aggravate cancer outcomes. The data thus carry high impact for researchers, funders, and policymakers alike.

Keywords
Cancer, obesity, high-fat diet, Tp53, Tp53^{R270H}, Li-Fraumeni

INTRODUCTION

Obesity is a chronic metabolic condition characterized by elevated body weight, adiposity, and numerous comorbidities, including cardiovascular disease, diabetes and autoimmunity. Obesity (and more moderate 'overweight') affect ~1.3 billion individuals globally, and the direct economic costs in the US alone are estimated at $173 billion per year[1]. In addition to cardiometabolic complications, obesity associates with increased incidence and severity of multiple cancers, including at 13 distinct anatomical sites[2-5]. Obesity has also been associated with altered treatment efficacy and toxicity[6,7]. Further, Obesity correlates with higher recurrence rates and poorer cancer prognoses[8], findings that have led to the inclusion of weight management in clinical guidelines for cancer survivors[9-11].

While numerous mechanisms have been proposed to explain how obesity may drive cancer[12-16], and translationally relevant understanding remains elusive. Fundamental questions remain, including "To through which mechanisms, does obesity influence tumorigenesis?" and "When, where, and with cancer types does obesity exacerbate (or inhibit) tumorigenesis." This lack of understanding derives from methodological issues, questions of reverse causality, detection and selection biases, and the overall breadth of distinct cancers observed in the clinic[17,18]. In these contexts, an accurate research record (literature) is critical to the development of effective clinical practice, policymaking, and research prioritization. Negative findings represent a vital part of the research record, one that is often underreported. Thus 'publication bias'[19] carries real-life consequences for patients, both indirect and direct (in the case of clinical trials)[20]. Given the overall limited understanding of the mechanistic links between obesity and cancer, publication of negative data is therefore essential. One challenge that exists well before publication is that investigators are typically not motivated, nor do they have substantial professional incentives, to complete fully powered studies once pilot data suggest weak or absent phenotypes; this is especially true for the very long-term (and resource intensive) studies that comprise much of cancer research. With respect to the link between obesity and cancer, recent literature does contain select reports that question the causal association between body mass index (BMI) and reduced cancer survival[21-31].

In this study, we tested the interaction between chronic high fat feeding in mice and a Tp53- model of spontaneous multi-cancer syndrome (MCS) (the *Tp53*$^{R270H/+}$ mouse). *TP53* is one of the most commonly mutated tumor suppressor genes in human cancers[32] and hotspot mutations cause Li-Fraumeni syndrome (LFS)[33-35]. LFS is an autosomal dominant disorder characterized by a marked susceptibility to diverse TP53 dependent cancers. *Tp53*$^{R270H/+}$ mice (the equivalent of the human Li-Fraumeni hotspot mutation R273H) faithfully recapitulate many aspects of the human MCS disorder, exhibiting a broad spectrum of tumors, including a variety of carcinomas, soft tissue and bone sarcomas, leukemia, and even glioblastoma (the most common brain cancer in LFS patients), with a mean survival time of just over one year.

High-fat diet (HFD) feeding is the most commonly used murine model of obesity[36,37]. The utility of the model is underpinned by human epidemiological studies that associate increased dietary fat

intake with obesity incidence[38-40]. Elevated dietary fat intake in humans (and in HFD mice) increases adiposity and associated hyperglycemia, inflammation, hypertension, plasma lipids, insulin resistance, and reduced beta-cell function[41]. Over time, this collectively leads to 'metabolic syndrome' characterized by elevated adiposity, cardiovascular disease, hepatosteatosis, type 2 diabetes, and increased mortality[42,43]. Importantly, HFD treatment is just one of many murine models of human obesity (and modern Western diet composition). Just as human obesity is increasingly acknowledged as a heterogeneous set of disorders with numerous distinct genetic, epigenetic, and environmental drivers, HFD treatment models only a small subset of known drivers of human obesity.

Here, we report a deep longitudinal analysis of two large cohorts of *Tp53*$^{R270H/+}$ animals chronically challenged with HFD or control chow diet (CD). Surprisingly, despite rapid and highly penetrant induction of obesity and associated metabolic sequelae, we find no effect of HFD on overall survival, tumor burden, or tumor spectrum. The data highlight an important example where chronic obesity does not accelerate or aggravate cancer etiology, and identify a novel negative control for the field.

RESULTS

A cohort to study chronic effects of obesity on *Tp53*-dependent cancers.

We set up a cohort of ~400 animals, with equal representation of females and males. The cohort included 203 *Tp53*$^{R270H/+}$ animals and 156 wildtype (WT) littermates to control for potential developmental effects[44]. All mice were fed chow diet (CD) until 8 weeks of age, when they were randomly assigned to CD or high-fat diet (HFD) for the remainder of the experiment. We tracked animals from birth to endpoint (70 weeks of age; >1 year of HFD) regularly monitoring morphological, growth and metabolic characteristics, as well as performing health checks for signs of cancer onset 2-3 times per week (**Fig.1A**). At sacrifice, all animals underwent a 21-organ dissection protocol in which tissues were isolated, processed for histology, and scored by a board-certified pathologist.

Mice of both genotypes and sexes responded rapidly and consistently to the HFD intervention with significant gains in overall fat and whole-body mass, compared to controls (**Fig.1B, Fig.S1A**). Notable given previous reports of metabolic roles for Tp53, we found no significant differences in HFD-triggered body or fat mass accumulation in *Tp53*$^{R270H/+}$ compared to WT animals (**Fig.S1B**). Histopathological evaluation revealed increased immune infiltration, lipoblast activity (indicative of adipose tissue proliferation), adipocyte size and adipocyte shape heterogeneity in HFD-treated animals (**Fig.1C**). Plasma metabolomics analysis at 8 weeks (immediately before HFD-feeding), 16 weeks of age (8 weeks into the diet regimen) and 40 weeks of age (32 weeks into diet regimen) revealed a substantial number of consistent changes in polar and non-polar metabolites (**Fig.1D**).

Thus, we generated a large-scale cohort for assessing interaction between HFD-induced obesity and *Tp53*$^{R270H/+}$ induced cancer. The data demonstrate that the *Tp53*$^{R270H/+}$ mutation does not impact the physiological response to HFD.

HFD does not alter survival in *Tp53*$^{R270H/+}$ mice.

Animals were therefore challenged with HFD and obesity, on average, for greater than one year (range: 6-62 weeks). To our surprise, we did not observe any change in survival probability upon HFD treatment. *Tp53*$^{R270H/+}$ animals under CD or HFD showed near-identical median survival times around 64-65 weeks of age (**Fig.2A**). No indication of potentially confounding heterogeneity effects was observed (e.g. altered shape of the Kaplan-Meier curve). The lack of difference in survival held true for both females and males (**Fig.S2A**), and importantly, it held true for separate discovery and validation cohorts run ~2 years apart (**Fig.S2B**). The discovery cohort was run and analyzed before the COVID19 pandemic, and the validation cohort, after. Both included at least 14 animals per sex and diet; animals from the two cohorts were derived from distinct sets of breeding pairs and were challenged with HFD/CD from distinct manufacturer batches. These data demonstrate a reproducible lack of effect of chronic HFD on *Tp53*$^{R270H/+}$ survival. Thus, *Tp53*$^{R270H/+}$-triggered cancer outcome is largely refractory to the metabolic and pathophysiological alterations induced by high-fat diet.

HFD shows minimal impact on tumor burden, prevalence and spectrum in *Tp53*$^{R270H/+}$ mice.

True to the model, *Tp53*$^{R270H/+}$ mutants often exhibited multiple primary tumors per animal. Survival aside, we therefore also tested if HFD-triggered obesity might impact tumor burden on a per animal basis. Remarkably, tumor burden also did not differ between HFD- and CD-fed animals (**Fig.2B**). Both groups showed tumor burdens ranging from zero to five primary tumors per animal and no significant difference was detected between HFD- and CD-fed groups (**Fig.2B**). This observation held for independent analyses of female and male animals (**Fig.S2C**). Thus, chronic HFD-induced obesity does not appreciably impact tumor burden in *Tp53*$^{R270H/+}$ mice.

As indicated, Li Fraumeni syndrome and the *Tp53*$^{R270H/+}$ model are characterized by heightened cancer incidence across a range of tumor types, and a wide range of targeted tissues. Where the sufficiently powered, we also tested for HFD-induced changes in tumor type. Consistent with literature[35], the majority of tumors in *Tp53*$^{R270H/+}$ animals were carcinomas and sarcomas, followed by leukemias and lymphomas (**Fig.2C**). Primary sites for tumor emergence included the reproductive system (prostate, uterus, seminal vesicles), bone and bone marrow, lungs, esophagus, skin, thymus, and soft tissues (**Fig.2D**). While modest tendencies towards one or the other tumor type cannot be definitively ruled out, we found no significant evidence of changed tumor type (carcinoma and sarcoma) comparing HFD-treated *Tp53*$^{R270H/+}$ animals with those on chow (**Fig.2C**). Once again, these observations were true for both females and males (**Fig.S2D**). The large cohort size notwithstanding, the study was not powered to detect differences in targeted tissues (**Fig.S2E**).

Thus, *Tp53*$^{R270H/+}$-dependent cancers are largely refractory to the effects of HFD-induced obesity.

DISCUSSION

Overall, our data provide a clear example where obesity and HFD-induced metabolic changes have limited impact on tumorigenesis and cancer outcomes. This finding is significant in the context of known publication bias against negative data[19]. Further, our study offers empirical evidence (that leverages the power of isogenicity and environmental control) supporting epidemiological data showing little to no association between obesity and select human cancers[21-31].

Notably, the question of when obesity does, and does not, associate with cancer is exacerbated by an underappreciation for the heterogeneity of human obesity itself. Our work[44-46] and that of many others[47-49] have highlighted that obesity is an umbrella term for what are a collection of disorders. Heterogeneous clinical presentations include metabolically 'healthy' and 'unhealthy' obesities, Types-A and -B obesities[46], and a complex intersection of clinically relevant heterogeneity in body size, shape and composition[50-52]. While our work highlights a negative interaction between HFD-induced obesity and *Tp53*$^{R270H/+}$ cancers, this does not mean that other subtypes of obesity (ie. distinct patient subsets) will not exhibit a strong interaction. Testing causal links between myriad obesity subtypes, across myriad cancer types, comprises a state-of-the-art challenge for the field.

The data also beg the equally large questions whether select cancer etiologies mechanistically uncoupled from HFD-modulated processes (adiposity, metabolite levels, insulin resistance, inflammation, etc.), and/or, whether select oncogene-induced etiologies are exquisitely robust to dietary influence. One hypothesis why *Tp53*$^{R270H/+}$ -triggered cancer might resist HFD-induced modulation, is that the *Tp53*$^{R270H/+}$ mutation triggers metabolic effects that counteract those driven by HFD. Indeed, Tp53 has been shown to be a significant regulator glycolysis, oxidative phosphorylation, amino acid and lipid metabolism[53,54,55], processes that have all been linked to tumors suppression in mice[56]. Along similar lines, adipose-tissue specific deletion of TP53 (*Tp53*$^{fl/fl}$*; Fabp4-Cre*) has been shown to normalize insulin sensitivity, glucose tolerance, and cytokine misexpression in obesity-prone agouti mice (Ay), and, to correlate with decreased senescence-like features[57]. In line with these studies (and related metabolic changes reported in Li-Fraumeni syndrome[58]) partial inhibition of fatty acid oxidation has been shown to delay cancer onset in *Tp53*$^{R270H/+}$ mice[59,60].

Beyond Tp53, this study identifies a new model for examining long-term tumor and host dynamics (genetic, transcriptional, immune, epigenetic and metabolic) in contexts of combined cancer susceptibility and metabolic disease evolution. The uncoupling of dietary effects from an altered cancer trajectory affords unique interdisciplinary opportunities to understanding chronic cancer and metabolic disease co-evolution (for up to ~1yr). Our own study products can support such studies. A biobank worth of bio samples will be stored long-term and are available upon request. In those regards, the study systematically catalogued myriad experimental variables including husbandry (parental IDs, litter sizes, littermate IDs) and controlled numerous potential metabolic confounders including housing density.

METHODS

Origin and maintenance of mice

This research complies with ethical regulations and protocols approved by Institutional Animal Care and Use Committee (Van Andel Institute, USA; protocols 19-0026, 22-09-036, 18-10-028, and 21-08-023). *B6.129S4-Trp53<tm3.1Tyj>/J* (*Tp53*$^{+/R270H}$) animals were originally generated in the Jacks lab[35] and purchased from Jackson Laboratories (stock #008182). Mice were backcrossed for over 10 generations and maintained in house by breeding with wild-type siblings and periodic background refreshment using wild-types from JAX. 392 F1 hybrids were generated by crossing 8-week-old *FVB.J* males with two 8-week-old *B6.Tp53*$^{R270H/+}$ females, which were separated after plug checking the next morning. Mating animals were randomly selected. All animals were fed breeder chow (Lab diet, 5021 cat. #0006540) *ad libitum* upon weaning and then randomly assigned to breeder chow or high-fat diet (Research diets, D12492i) at 8 weeks of age. Mice were housed in individually ventilated cages (Tecniplast, Sealsafe Plus GM500 in DGM Racks) at a density of maximum five animals per cage. Each cage was enriched with Enviro-dri (The Andersons, Crink-l'Nest) and cardboard dome homes (Shepherd, Shepherd Shack Dome). Whenever possible, same-sex siblings and same-sex animals from different litters were combined (~20 days of age). Animals were kept on a 12-hour light/dark cycle at an average ambient temperature of 23°C and 35% humidity.

Body composition data was collected from 359 animals, including 173 males (74 WT and 99 *Tp53*$^{+/R270H}$) and 186 females (82 WT and 104 *Tp53*$^{+/R270H}$). Chow diet (CD, Lab diet, 5021 cat. #0006540) or high-fat diet (HFD, Research diets, D12492i) was randomly assigned at 8 weeks of age, as follows: 24 WT males under CD, 29 WT males under HFD, 38 *Tp53*$^{+/R270H}$ males under CD, 56 *Tp53*$^{+/R270H}$ males under HFD, 30 WT females under CD, 40 WT females under HFD, 41 *Tp53*$^{+/R270H}$ females under CD, and 60 *Tp53*$^{+/R270H}$ females under HFD. At 4, 8, 16, 32, 40, 50, 60, and 70 weeks of age (or at euthanasia), mice were weighed and scanned via EchoMRI for fat and lean mass composition in the morning (EchoMRI™, EchoMRI™-100H).
Tumor analysis was conducted on 182 animals: 85 males (7 WT-CD, 10 WT-HFD, 26 *Tp53*$^{+/R270H}$-CD, and 42 *Tp53*$^{+/R270H}$-HFD) and 97 females (8 WT-CD, 13 WT-HFD, 30 *Tp53*$^{+/R270H}$-CD, and 46 *Tp53*$^{+/R270H}$-HFD). We performed tumor analysis blinded for genotype and phenotype, temporally collecting mice according to the timing of health reports. We specify in the text every time we are only referring to one of the sexes.

Statistics and reproducibility

Power analysis was performed by the Van Andel Institute (VAI) Bioinformatics and Biostatistics Core using the pwr R package for Power Analysis (R v. 3.5.2)[61], to determine sample size. In particular a 2 sample test of proportions was run based on an estimated effect size calculated on published data[35] using a firth logistic regression. Power was set to 80%, alpha = 0.05, and assuming each group having equal sample sizes, considering 2 treatments (CD and HFD) and 5 different types of cancer evaluated (carcinoma, sarcoma, lymphoma, and leukemia).

Due to COVID-related reductions, 165 animals were randomly excluded for tumor analysis. Additionally, 7 mice died after birth, precluding further analysis. 10 were found dead and too stiff to harvest. The final cohort included all animals from litters of 5-12 pups.
Experiments were randomized, and investigators were blinded to group allocation and outcome assessment wherever possible.

Genotyping
Ear punch biopsies were collected at 10 days and digested in 20 µl genomic DNA lysis buffer (100 mM Tris-HCl pH 8.5, 5 mM EDTA, 0.2% SDS, 100 mM NaCl) with 20 mg proteinase K (Thermo Scientific, EO0491). The thermal cycling protocol used was 55°C for 16 hours, 95°C for 10', and a 4°C hold (lid at 105°C). Nuclease-free water (Invitrogen, AM9938) was added to each lysate for a final volume of 180 µl. PCR reactions for *Tp53* allele used 1 µl diluted biopsy lysate in a 19 µl master mix (1X DreamTaq Buffer, 0.2 mM dNTPs, 0.1 µM primer forward and reverse mix, 2 U DreamTaq DNA Polymerase, in nuclease-free water; Thermo Scientific, EP0703). PCR primer and thermal cycling conditions are detailed in Supplementary Tables 1 and 2. 20 µl of each PCR product were digested with 0.5 µl MslI (for $Tp53^{R270H/+}$; New England BioLabs, R0571L) in a final reaction volume of 30 µl. Restriction conditions are detailed in Supplementary Table 3. Digestion products (~500 bp WT *Tp53*, ~200 + ~300 bp $Tp53^{R270H/+}$) were visualized on a 3% agarose gel (Fisher Scientific, BP160-500) in 1X TAE, with GelRed as intercalating dye (Biotium, 41003).

Health monitoring
VAI Vivarium Core staff monitored mice 2-3 times per week for health, well-being, and abnormal mass/tumor presence. Mice were euthanized if they exhibited >20% weight loss, tumors ~15% of body weight (this maximal tumor size was never exceeded), tumor ulcerations, tumor discharge or hemorrhage, mobility issues, reduced appetite or hydration, limited defecation or urination, abnormal gait or posture, labored breathing, lack of movement, or hypothermia. Mice with reported health concerns or those reaching the 70-week study endpoint were euthanized via CO_2 asphyxiation and cervical dislocation.

Tissue harvesting
Tissues were dissected and fixed in 10% NBF solution (3.7-4% formaldehyde 37-40%, 0.03 M NaH_2PO_4, 0.05 M Na_2HPO_4, in distilled water with final pH of 7.2± 0.5): epidydimal white adipose tissue (eWAT); uterus or preputial glands, seminal vesicles, and testis; bladder; pancreas; spleen; intestine; stomach; mesenteric fat; liver; kidneys; heart; lungs; thymus; brain; breast (9th); hindlimb muscles and bones. We also recovered spine, ribs, skull, skin, and any other mass if abnormal. Fixative volume was 15-20 times the tissue volume. Specimens > 2.5 mm thick were cut to proper fixation. Most tissues were fixed for 40 hours, while fat-rich tissues (eWAT, mesenteric fat, uterus) were fixed for 72 hours. Bones and spines were fixed for 1 week followed by 1-week decalcification in 14% EDTA (14% free-acid EDTA at pH 7.2, adjusted with NH_4OH). After incubation, all tissues were moved to 70% ethanol. Data collection was blinded.

Tissue preparation for histology

All tissues were paraffin-embedded by the VAI Pathology and Biorepository Core. Dehydration and clearing were automated with a Tissue-Tek VIP 5 (Sakura) using the following protocol: 60' in 70% ethanol; 60' in 80% ethanol; 2x 60' in 95% ethanol; 3x 60' in 100% ethanol; 2x 30' in xylene; and 75'in paraffin. Embedding was performed with a Leica EG1150. Three 5-µm sections, spaced 150 µm apart, were cut from each tissue for hematoxylin and eosin (H&E) staining using a Leica rotary microtome. The remaining tissue was stored as a paraffin block. H&E staining was performed with a Tissue-Tek Prisma Plus Automated Slide Stainer (Sakura) and Prisma H&E Staining Kit #1.

Pathology evaluation

Standard 5-µm H&E-stained sections were assessed for tumors and dysplastic lesions by a board-certified pathologist at the VAI Pathology and Biorepository Core. Most samples were provided blindly. Tumors were classified as malignant or benign, with all malignant tumors being primary. Metastatic or secondary tumors were identified based on primary tumor characteristics and immunohistochemical validation but were not reported in this study. Tumors were categorized into carcinomas, germ cell tumors, leukemias, lymphomas, and sarcomas, with detailed classification by tissue of origin.

Plasma collection

Blood was collected from animals at 8, 16, and 40 weeks of age by tail nicking directly harvesting in EDTA-coated Microvettes (Sarstedt, 16.444.100) to reduce hemolysis, which were placed on ice immediately after collection. Plasma was separated by centrifugation within one hour of collection, at 4000 g for 10' in a pre-cooled centrifuge (4°C). The supernatant was collected in pre-cooled 1.5 ml receiving tubes and snap-frozen in liquid nitrogen. Plasma was then placed at -80°C for long-term storage.

Metabolite and lipid extraction

Polar metabolites and lipids were separated by mixing 40uL of plasma in 1mL of chloroform:methanol:water (2:2:1.8 v/v) (PMID: 13671378, PMID: 38987243), incubating on wet ice for one hour, and centrifugation at 14000xg for 10 minutes to induce phase separation. 495µL and 100µL of the upper aqueous and bottom organic layers, respectively, were collected into separate tubes and dried in a speedvac. The aqueous layer was resuspended 100µL of water for metabolomics analysis. The organic layer was resuspended 200µL of 50:50 (isopropanol:acetonitrile, v/v) for metabolomics analysis.

Metabolomics analyses

Metabolomics samples were analyzed with a Thermo Vanquish dual liquid chromatography system utilizing two alternating methods, referred to as Chromatography 1 and Chromatography 2, coupled to an Orbitrap ID-X (Thermo Fisher Scientific) using an H-ESI (heated electrospray

ionization) source in positive and negative mode respectively. 2 µL of each standard and/or sample was injected, column temperatures were kept at 40 °C, and flow rate was held at 0.4 mL/min. For both chromatography 1 and 2, mobile phase A consisted of 100% LC/MS grade water (W6, Fisher), 0.1% LC/MS grade formic acid (A117, Fisher Scientific), and Mobile phase B consisted of 99% LC/MS grade acetonitrile (A955, Fisher Scientific), 1% LC/MS grade water, 0.1% LC/MS grade formic acid. Chromatography 1 used a 13-minute reversed-phase chromatography Cortecs T3 column (1.6 µm, 2.1mm × 150mm, 186008500, Waters, Eschborn, Germany) combined with a VanGuard pre-column (1.6 µm, 2.1 mm × 5 mm, 186008508, Waters), and the gradient was as follows: 0-1 min held at 0% B, 1-11 min from 0% B to 100% B, and 11-13 min held at 100% B. A 13-minute wash gradient was run between every injection (in parallel with chromatography 2) to flush the column and to re-equilibrate solvent conditions as follows: 0-5 min held at 100% B, 5-5.5 min from 100% B to 0% B, and 5.5-13 min held at 0% B. Chromatography 2 used a 13-minute reversed-phase chromatography Acquity Premier CSH phenyl-hexyl column (1.7 µm, 2.1mm × 150mm, 186009479, Waters) combined with a VanGuard cartridge (1.7 µm, 2.1 mm × 5 mm, 186009480, Waters), and the gradient was as follows: 0-0.5 min held at 1% B, 0.5-4 min from 1% B to 25% B, 4-4.5 min held at 25% B, 4.5-11 min from 25% B to 100% B, and 11-13 min held at 100% B. A 13-minute wash gradient was run between every injection (in parallel with chromatography 1) to flush the column and to re-equilibrate solvent conditions as follows: 0-5 min held at 100% B, 5-5.5 min from 100% B to 1% B, and 5.5-13 min held at 1% B. For Chromatography 1, the mass spectrometer parameters were: source voltage 3500V, sheath gas 60, aux gas 19, sweep gas 1, ion transfer tube temperature 300°C, and vaporizer temperature 250°C. Full scan data were collected using the orbitrap with a scan range of 105-1000 m/z at a resolution of 120,000 and RF lens at 60%. For Chromatography 2, the mass spectrometer parameters were: source voltage -2500V, sheath gas 70, aux gas 25, sweep gas 1, ion transfer tube temperature 300°C, and vaporizer temperature 250°C. Full scan data were collected using the orbitrap with a scan range of 70-1000 m/z at a resolution of 120,000 and RF lens at 35%. Both chromatographies utilized the same methodology for data dependent MS2 fragmentation which induced in the orbitrap using assisted higher-energy collisional dissociation (HCD) collision energies at 20, 35, and 50% as well as with collision-induced dissociation (CID) at a collision energy of 30%. For both MS2 fragmentations, orbitrap resolution was 30,000, the isolation window was 1.5 m/z, and total cycle time was 0.6 sec.

Lipidomics analyses

Lipidomics samples were analyzed with a Thermo Vanquish dual liquid chromatography system utilizing two alternating methods, referred to as Chromatography 1 and Chromatography 2, coupled to an Orbitrap ID-X (Thermo Fisher Scientific) using an H-ESI (heated electrospray ionization) source in positive and negative mode respectively. 2 µL of each standard and/or sample was injected, column temperatures were kept at 50 °C, and flow rate was held at 0.4 mL/min. For both chromatography 1 and 2, mobile phase A consisted of 60% LC/MS grade acetonitrile (A955, Fisher Scientific), 40% LC/MS grade water (W6, Fisher Scientific), 0.1% LC/MS grade formic

acid (A117, Fisher Scientific), 10mM ammonium formate (70221, Fisher Scientific), and mobile phase B consisted of 90% LC/MS grade isopropanol (A461, Fisher Scientific), 8% LC/MS grade acetonitrile, 2% LC/MS grade water, 0.1% LC/MS grade formic acid, and 10mM ammonium formate. Chromatography 1 used a 30-minute reversed-phase chromatography Accucore C30 column (2.6 µm, 2.1 mm x 150 mm, 27826-152130, Thermo Fisher Scientific) combined with an Accucore C30 guard column (2.6 µm, 2.1mm x 10 mm, 27826-012105, Thermo Fisher Scientific), and the gradient was as follows: 0-1 min held at 25% B, 1-3 min from 25% B to 40% B, 3-19 min from 40% B to 75% B, 19-20.5 min 75% B to 90% B, 20.5-28 min from 90% B to 95% B, 28-28.1 min from 95% B to 100% B, and 28.1-30 min held at 100% B. A 30 minute wash gradient was run between every injection (in parallel with chromatography 2) to flush the column and to re-equilibrate solvent conditions as follows: 0-2 min held at 100% B and 0.3 mL/min, 2-2.1 min from 100% B to 25% B and held at 0.3 mL/min, 2.1-4 min held at 25% B and ramp to 0.4 mL/min, 4-6 held at 25% B and ramp to 0.6 mL/min, 6-17 min held at 25% B and 0.6 mL/min, 17-17.1 min held at 25% B and ramp to 0.4 mL/min, and 17.1-30 min held at 25% B and 0.4 mL/min. Chromatography 2 used a 30-minute reversed-phase chromatography Acquity UPLC CSH C18 column (1.7 µm, 2.1 mm × 100 mm, 186005297, Waters, Eschborn, Germany) combined with a a VanGuard pre-column (1.7 µm, 2.1 mm × 5 mm, 186005303, Waters), and the gradient was as follows: 0-1 min held at 25% B, 1-3 min from 25% B to 40% B, 3-4 min from 40% B to 50% B, 4-16 min from 50% B to 65% B, 16-17 min from 65% B to 70% B, 17-25 min from 70% B to 75% B, 25-27 min from 75% B to 100% B, and 27-30 min held at 100% B. A 30-minute wash gradient was run between every injection (in parallel with chromatography 1) that used the same gradient as chromatography 1 wash gradient. For both methods mass spectrometer parameters were: source voltage +3250V or -3000 depending on method polarity, sheath gas 40, aux gas 10, sweep gas 1, ion transfer tube temperature 300°C, and vaporizer temperature 275°C. Full scan data were collected using the orbitrap with a scan range of 200-1700 m/z at a resolution of 500,000 and RF lens at 45%. Data dependent MS2 fragmentation was induced in the orbitrap using assisted higher-energy collisional dissociation (HCD) collision energies at 15, 30, 45, 75, and 110% as well as with collision-induced dissociation (CID) at a collision energy of 35%. For both MS2 fragmentations, orbitrap resolution was 15,000 and the isolation window was 1.5 m/z. A m/z 184 mass trigger, indicative of phosphatidylcholines, was used for CID fragmentation. Data dependent MS3 fragmentation was induced in the ion trap with scan rate set at Rapid using CID at a collision energy of 35%. MS3 scans were triggered by specific acyl chain losses for detailed analysis of mono-, di-, and triacylglycerides. Total cycle time was 2 sec. Lipid identifications were assigned using LipidSearch (v5.0, Thermo Fisher Scientific).

ACKNOWLEDGEMENTS

We thank current and former members of the lab for their experimental support, including A. Drougard, M. McDonald, B. Grimaldi, A. Parham, A. Bergsma, J. Richards, R. Schuitema, C.H. Yang, V. Wegert, M. Edozie, D. Aicher, K. Schaefer, and Y. Liu. We thank T. Yang, R. Jones, B, Williams, E. Lien, C. Essenburg, N. Vander Schaaf, P. Stevens, L. DeCamp, E. Levine, E. Ma, D.

Lu, H. Lu, V. Molchanov, and J. Endicott for suggestions and support; as well as the MPI-IE Facilities and VAI Vivarium (in particular, B. Eagleson, S. Bechaz, A. Rapp, R. Burdette, E. Tubbergen, E. Hamel, M. Powers, and S. Greenwald; RRID:SCR_023211); Transgenics (in particular, T. Kempston, and A. Guikema; RRID:SCR_022914); Pathology and Biorepository (in particular, S. Jewell, D. Rohrer, B. Berghuis, L. Turner, S. Whitford, A. Bouwman, K. Feenstra, and K. Goudreau; RRID:SCR_022912); Bioinformatics and Biostatistics (RRID:SCR_024762), Mass Spectrometry (in particular, R. Sheldon, A. Ellis, C. Isaguirre, M. Vincent; RRID:SCR_024903), and Optical Imaging (in particular, C. Esquibel, K. Gallik, and L. Cohen; RRID:SCR_021968) Cores. This work was supported by funding from the MPG, the ERC and VAI through internal philanthropy to JAP, NIH award number 1R01HG012444 to JAP and JHN, MeNU pilot project grants and Human Frontier Science Program Long-Term Fellowship LT000441/2018-L to IP. The funders had no role in study design, data collection and analysis, decision to publish or preparation of the manuscript.

AUTHOR CONTRIBUTIONS

IP and JAP conceived the project, designed the overall methodology, and supervised the work. IP designed each individual experiment, performed the *in vivo* experiments, genotyping and the tissue harvesting together with MT. IP analyzed all the phenotypic data, while LF and SA supported data analysis. GH performed all the pathology reviews. IP and ZM performed statistical analyses. IP and JAP wrote, reviewed and edited the original draft. IP prepared the figures. JAP and IP acquired funds. JAP provided resources for the experiments.

COMPETING INTERESTS STATEMENT

The authors declare no competing interests.

REFERENCES

1 Ward, Z. J., Bleich, S. N., Long, M. W. & Gortmaker, S. L. Association of body mass index with health care expenditures in the United States by age and sex. *PLOS ONE* **16**, e0247307 (2021). https://doi.org:10.1371/journal.pone.0247307

2 Renehan, A. G., Tyson, M., Egger, M., Heller, R. F. & Zwahlen, M. Body-mass index and incidence of cancer: a systematic review and meta-analysis of prospective observational studies. *The Lancet* **371**, 569-578 (2008). https://doi.org:10.1016/S0140-6736(08)60269-X

3 Bhaskaran, K. *et al.* Body-mass index and risk of 22 specific cancers: a population-based cohort study of 5·24 million UK adults. *The Lancet* **384**, 755-765 (2014). https://doi.org:10.1016/S0140-6736(14)60892-8

4 Moore, L. L., Chadid, S., Singer, M. R., Kreger, B. E. & Denis, G. V. Metabolic Health Reduces Risk of Obesity-Related Cancer in Framingham Study Adults. *Cancer Epidemiology, Biomarkers & Prevention* **23**, 2057-2065 (2014). https://doi.org:10.1158/1055-9965.Epi-14-0240

5 Mahamat-saleh, Y. *et al.* Association of metabolic obesity phenotypes with risk of overall and site-specific cancers: a systematic review and meta-analysis of cohort studies. *British Journal of Cancer* (2024). https://doi.org:10.1038/s41416-024-02857-7
6 Lauby-Secretan, B. *et al.* Body Fatness and Cancer--Viewpoint of the IARC Working Group. *N Engl J Med* **375**, 794-798 (2016). https://doi.org:10.1056/NEJMsr1606602
7 Marinac, C. R. *et al.* Body mass index throughout adulthood, physical activity, and risk of multiple myeloma: a prospective analysis in three large cohorts. *Br J Cancer* **118**, 1013-1019 (2018). https://doi.org:10.1038/s41416-018-0010-4
8 Petrelli, F. *et al.* Association of Obesity With Survival Outcomes in Patients With Cancer: A Systematic Review and Meta-analysis. *JAMA Network Open* **4**, e213520-e213520 (2021). https://doi.org:10.1001/jamanetworkopen.2021.3520
9 Ligibel, J. A. *et al.* American Society of Clinical Oncology position statement on obesity and cancer. *J Clin Oncol* **32**, 3568-3574 (2014). https://doi.org:10.1200/jco.2014.58.4680
10 Rock, C. L. *et al.* Nutrition and physical activity guidelines for cancer survivors. *CA: A Cancer Journal for Clinicians* **62**, 242-274 (2012). https://doi.org:https://doi.org/10.3322/caac.21142
11 Senkus, E. *et al.* Primary breast cancer: ESMO Clinical Practice Guidelines for diagnosis, treatment and follow-up†. *Annals of Oncology* **24**, vi7-vi23 (2013). https://doi.org:https://doi.org/10.1093/annonc/mdt284
12 Font-Burgada, J., Sun, B. & Karin, M. Obesity and Cancer: The Oil that Feeds the Flame. *Cell Metabolism* **23**, 48-62 (2016). https://doi.org:10.1016/j.cmet.2015.12.015
13 Perry, R. J. & Shulman, G. I. Mechanistic Links between Obesity, Insulin, and Cancer. *Trends in Cancer* **6**, 75-78 (2020). https://doi.org:10.1016/j.trecan.2019.12.003
14 Li, R. *et al.* Transcriptome and DNA Methylome Analysis in a Mouse Model of Diet-Induced Obesity Predicts Increased Risk of Colorectal Cancer. *Cell Reports* **22**, 624-637 (2018). https://doi.org:10.1016/j.celrep.2017.12.071
15 Calabrese, C. *et al.* Lipids and adipocytes involvement in tumor progression with a focus on obesity and diet. *Obes Rev*, e13833 (2024). https://doi.org:10.1111/obr.13833
16 Engin, A. B. & Engin, A. Next-Cell Hypothesis: Mechanism of Obesity-Associated Carcinogenesis. *Adv Exp Med Biol* **1460**, 727-766 (2024). https://doi.org:10.1007/978-3-031-63657-8_25
17 Lysaght, J. & Conroy, M. J. The multifactorial effect of obesity on the effectiveness and outcomes of cancer therapies. *Nature Reviews Endocrinology* (2024). https://doi.org:10.1038/s41574-024-01032-5
18 Lennon, H., Sperrin, M., Badrick, E. & Renehan, A. G. The Obesity Paradox in Cancer: a Review. *Current Oncology Reports* **18**, 56 (2016). https://doi.org:10.1007/s11912-016-0539-4
19 Mlinarić, A., Horvat, M. & Šupak Smolčić, V. Dealing with the positive publication bias: Why you should really publish your negative results. *Biochem Med (Zagreb)* **27**, 030201 (2017). https://doi.org:10.11613/bm.2017.030201
20 Metcalfe, S. *et al.* Trastuzumab: possible publication bias. *The Lancet* **371**, 1646-1648 (2008). https://doi.org:10.1016/S0140-6736(08)60706-0
21 Hines, R. B. *et al.* Effect of comorbidity and body mass index on the survival of African-American and Caucasian patients with colon cancer. *Cancer* **115**, 5798-5806 (2009). https://doi.org:10.1002/cncr.24598
22 Navarro, W. H. *et al.* Effect of Body Mass Index on Mortality of Patients with Lymphoma Undergoing Autologous Hematopoietic Cell Transplantation. *Biology of Blood and Marrow Transplantation* **12**, 541-551 (2006). https://doi.org:https://doi.org/10.1016/j.bbmt.2005.12.033

23 Parker, A. S. *et al.* Greater body mass index is associated with better pathologic features and improved outcome among patients treated surgically for clear cell renal cell carcinoma. *Urology* **68**, 741-746 (2006). https://doi.org:https://doi.org/10.1016/j.urology.2006.05.024
24 Schlesinger, S. *et al.* Postdiagnosis body mass index and risk of mortality in colorectal cancer survivors: a prospective study and meta-analysis. *Cancer Causes & Control* **25**, 1407-1418 (2014). https://doi.org:10.1007/s10552-014-0435-x
25 Hakimi, A. A. *et al.* An Epidemiologic and Genomic Investigation Into the Obesity Paradox in Renal Cell Carcinoma. *JNCI: Journal of the National Cancer Institute* **105**, 1862-1870 (2013). https://doi.org:10.1093/jnci/djt310
26 Amptoulach, S., Gross, G. & Kalaitzakis, E. Differential impact of obesity and diabetes mellitus on survival after liver resection for colorectal cancer metastases. *Journal of Surgical Research* **199**, 378-385 (2015). https://doi.org:https://doi.org/10.1016/j.jss.2015.05.059
27 Brunner, A. M. *et al.* Association between baseline body mass index and overall survival among patients over age 60 with acute myeloid leukemia. *American Journal of Hematology* **88**, 642-646 (2013). https://doi.org:https://doi.org/10.1002/ajh.23462
28 Banack, H. R. & Kaufman, J. S. The obesity paradox: Understanding the effect of obesity on mortality among individuals with cardiovascular disease. *Preventive Medicine* **62**, 96-102 (2014). https://doi.org:https://doi.org/10.1016/j.ypmed.2014.02.003
29 Mayeda, E. R. & Glymour, M. M. The Obesity Paradox in Survival after Cancer Diagnosis: Tools for Evaluation of Potential Bias. *Cancer Epidemiology, Biomarkers & Prevention* **26**, 17-20 (2017). https://doi.org:10.1158/1055-9965.Epi-16-0559
30 Park, Y., Peterson, L. L. & Colditz, G. A. The Plausibility of Obesity Paradox in Cancer—Point. *Cancer Research* **78**, 1898-1903 (2018). https://doi.org:10.1158/0008-5472.Can-17-3043
31 Petrelli, F. *et al.* Obesity paradox in patients with cancer: A systematic review and meta-analysis of 6,320,365 patients. *medRxiv*, 2020.2004.2028.20082800 (2020). https://doi.org:10.1101/2020.04.28.20082800
32 Hollstein, M., Sidransky, D., Vogelstein, B. & Harris, C. C. p53 Mutations in Human Cancers. *Science* **253**, 49-53 (1991). https://doi.org:doi:10.1126/science.1905840
33 Jr., F. P. L. a. J. F. F. Soft-Tissue Sarcomas, Breast Cancer, and Other Neoplasms. *Annals of Internal Medicine* **71**, 747-752 (1969). https://doi.org:10.7326/0003-4819-71-4-747 %m 5360287
34 Guha, T. & Malkin, D. Inherited TP53 Mutations and the Li–Fraumeni Syndrome. *Cold Spring Harbor Perspectives in Medicine* **7** (2017). https://doi.org:10.1101/cshperspect.a026187
35 Olive, K. P. *et al.* Mutant p53 gain of function in two mouse models of Li-Fraumeni syndrome. *Cell* **119**, 847-860 (2004). https://doi.org:10.1016/j.cell.2004.11.004
36 Wang, C.-Y. & Liao, J. K. in *mTOR: Methods and Protocols* (ed Thomas Weichhart) 421-433 (Humana Press, 2012).
37 Buettner, R., Schölmerich, J. & Bollheimer, L. C. High-fat Diets: Modeling the Metabolic Disorders of Human Obesity in Rodents. *Obesity* **15**, 798-808 (2007). https://doi.org:https://doi.org/10.1038/oby.2007.608
38 George, V., Tremblay, A., Després, J. P., Leblanc, C. & Bouchard, C. Effect of dietary fat content on total and regional adiposity in men and women. *Int J Obes* **14**, 1085-1094 (1990).
39 Saris, W. H. M. *et al.* Randomized controlled trial of changes in dietary carbohydrate/fat ratio and simple vs complex carbohydrates on body weight and blood lipids: the CARMEN study. *International Journal of Obesity* **24**, 1310-1318 (2000). https://doi.org:10.1038/sj.ijo.0801451

40 Tucker, L. A. & Kano, M. J. Dietary fat and body fat: a multivariate study of 205 adult females. *The American Journal of Clinical Nutrition* **56**, 616-622 (1992). https://doi.org:https://doi.org/10.1093/ajcn/56.4.616
41 Rohm, T. V., Meier, D. T., Olefsky, J. M. & Donath, M. Y. Inflammation in obesity, diabetes, and related disorders. *Immunity* **55**, 31-55 (2022). https://doi.org:https://doi.org/10.1016/j.immuni.2021.12.013
42 Garaulet, M. & Madrid, J. A. Chronobiological aspects of nutrition, metabolic syndrome and obesity. *Adv Drug Deliv Rev* **62**, 967-978 (2010). https://doi.org:10.1016/j.addr.2010.05.005
43 Adams, K. F. *et al.* Overweight, obesity, and mortality in a large prospective cohort of persons 50 to 71 years old. *N Engl J Med* **355**, 763-778 (2006). https://doi.org:10.1056/NEJMoa055643
44 Panzeri, I. *et al.* Developmental priming of cancer susceptibility. *bioRxiv*, 2023.2009.2012.557446 (2023). https://doi.org:10.1101/2023.09.12.557446
45 Dalgaard, K. *et al.* Trim28 Haploinsufficiency Triggers Bi-stable Epigenetic Obesity. *Cell* **164**, 353-364 (2016). https://doi.org:10.1016/j.cell.2015.12.025
46 Yang, C.-H. *et al.* Independent phenotypic plasticity axes define distinct obesity sub-types. *Nature Metabolism* **4**, 1150-1165 (2022). https://doi.org:10.1038/s42255-022-00629-2
47 Coral, D. E. *et al.* A phenome-wide comparative analysis of genetic discordance between obesity and type 2 diabetes. *Nature Metabolism* **5**, 237-247 (2023). https://doi.org:10.1038/s42255-022-00731-5
48 Khera, A. V. *et al.* Polygenic Prediction of Weight and Obesity Trajectories from Birth to Adulthood. *Cell* **177**, 587-596.e589 (2019). https://doi.org:10.1016/j.cell.2019.03.028
49 Cirulli, E. T. *et al.* Profound Perturbation of the Metabolome in Obesity Is Associated with Health Risk. *Cell Metabolism* **29**, 488-500.e482 (2019). https://doi.org:https://doi.org/10.1016/j.cmet.2018.09.022
50 Petersen, M. C. *et al.* Cardiometabolic characteristics of people with metabolically healthy and unhealthy obesity. *Cell Metabolism* **36**, 745-761.e745 (2024). https://doi.org:10.1016/j.cmet.2024.03.002
51 Tabara, Y., Shoji-Asahina, A., Ogawa, A. & Sato, Y. Metabolically healthy obesity and risks of cardiovascular disease and all-cause mortality, a matched cohort study: the Shizuoka study. *International Journal of Obesity* **48**, 1164-1169 (2024). https://doi.org:10.1038/s41366-024-01541-3
52 Schulze, M. B. & Stefan, N. Metabolically healthy obesity: from epidemiology and mechanisms to clinical implications. *Nature Reviews Endocrinology* (2024). https://doi.org:10.1038/s41574-024-01008-5
53 Liu, Y., Su, Z., Tavana, O. & Gu, W. Understanding the complexity of p53 in a new era of tumor suppression. *Cancer Cell* **42**, 946-967 (2024). https://doi.org:10.1016/j.ccell.2024.04.009
54 Berkers, Celia R., Maddocks, Oliver D. K., Cheung, Eric C., Mor, I. & Vousden, Karen H. Metabolic Regulation by p53 Family Members. *Cell Metabolism* **18**, 617-633 (2013). https://doi.org:10.1016/j.cmet.2013.06.019
55 Liu, Y. & Gu, W. The complexity of p53-mediated metabolic regulation in tumor suppression. *Seminars in Cancer Biology* **85**, 4-32 (2022). https://doi.org:https://doi.org/10.1016/j.semcancer.2021.03.010
56 Li, T. *et al.* Tumor Suppression in the Absence of p53-Mediated Cell-Cycle Arrest, Apoptosis, and Senescence. *Cell* **149**, 1269-1283 (2012). https://doi.org:https://doi.org/10.1016/j.cell.2012.04.026

57 Minamino, T. *et al.* A crucial role for adipose tissue p53 in the regulation of insulin resistance. *Nature Medicine* **15**, 1082-1087 (2009). https://doi.org:10.1038/nm.2014
58 Wang, P.-Y. *et al.* Increased Oxidative Metabolism in the Li–Fraumeni Syndrome. *New England Journal of Medicine* **368**, 1027-1032 (2013). https://doi.org:doi:10.1056/NEJMoa1214091
59 Wang, P.-Y. *et al.* Reducing Fatty Acid Oxidation Improves Cancer-free Survival in a Mouse Model of Li-Fraumeni Syndrome. *Cancer Prevention Research* **14**, 31-40 (2021). https://doi.org:10.1158/1940-6207.Capr-20-0368
60 Wang, P.-y. *et al.* Inhibiting mitochondrial respiration prevents cancer in a mouse model of Li-Fraumeni syndrome. *The Journal of Clinical Investigation* **127**, 132-136 (2017). https://doi.org:10.1172/JCI88668
61 Champely, S., Ekstrom, C., Dalgaard, P., Gill, J., Weibelzahl, S., Anandkumar, A., Ford, C., Volcic, R., & De Rosario, H. *pwr: Basic functions for power analysis. Software*, <https://cran.r-project.org/web/packages/pwr/> (2017).

Fig.1

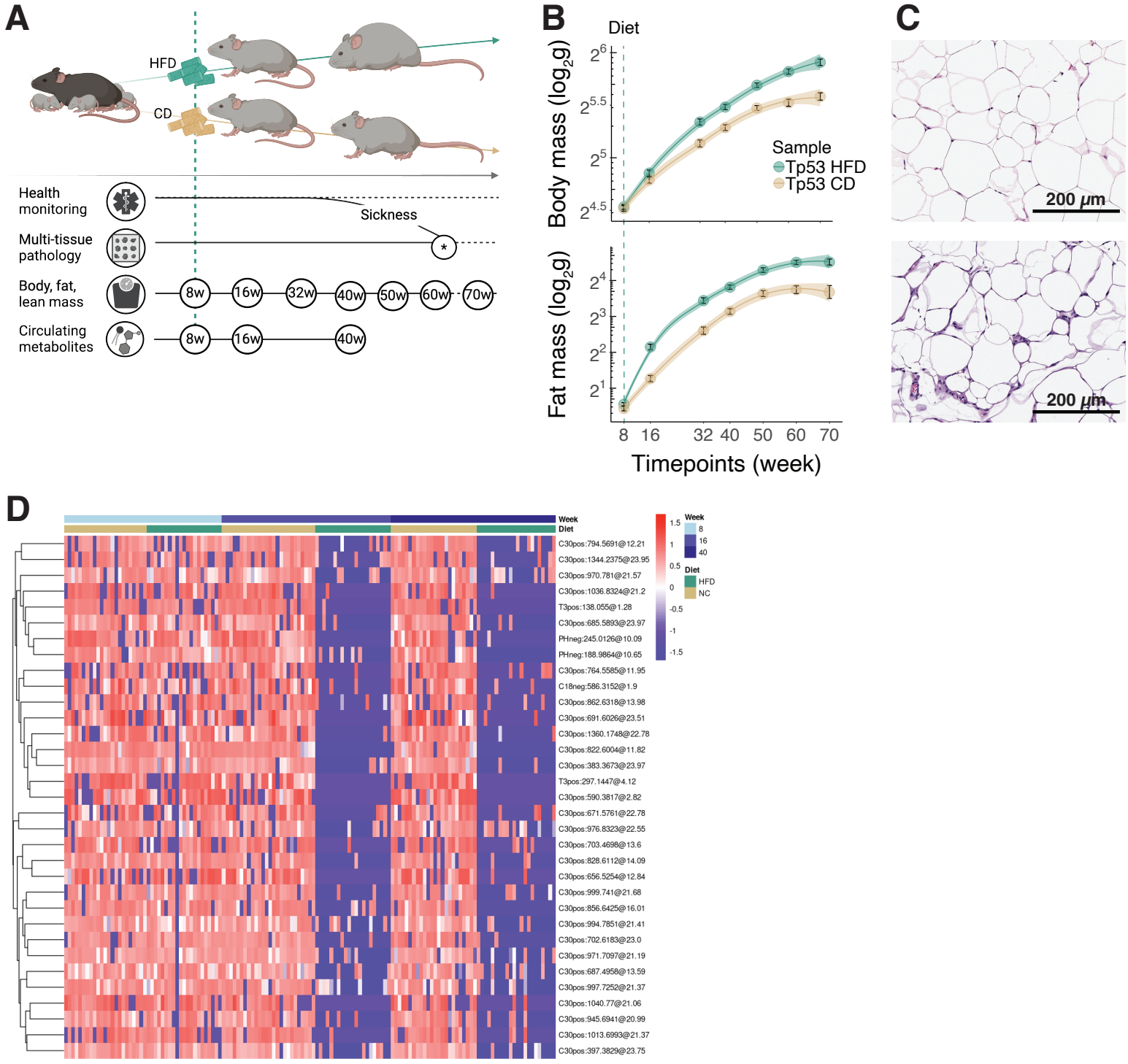
A
HFD
CD
Health monitoring
Sickness
Multi-tissue pathology
Body, fat, lean mass
8w
16w
32w
40w
50w
60w
70w
Circulating metabolites
B
Diet
Body mass (log2g)
Sample
Tp53 HFD
Tp53 CD
Fat mass (log2g)
Timepoints (week)
C
200 μm
D
Week
Diet
HFD
NC

Figure 1. A cohort to study chronic effects of obesity on *Tp53*-dependent cancers. A) Schematic of the experimental plan. *Tp53*$^{+/R270H}$ females were mated with the *Trim28*$^{+/D9}$ *FVB.J* males. F1 genotypes were screened for health issues and mass development. Tissues were harvested at sickness report. Histopathology determined the presence of tumors. Body, fat, and lean mass were measured at multiple timepoints. Blood was collected at multiple timepoints for metabolomic analysis. Created with BioRender.com. **B)** Scatter plots and smoothed conditional means (95% confidence interval, "loess" method) for *body* (top) and *fat* (bottom) mass in *Tp53*$^{+/R270H}$ females and males (pooled data). N=195 animals (101 females and 94 males). **C)** Representative examples of hematoxylin and eosin-stained adipose tissue from *chow*- (top) and *high-fat* (bottom) diet-fed *Tp53*$^{+/R270H}$ male animal at 70 weeks of age. N=1 animal. **D)** Heatmap of differentially abundant circulating metabolites between chow- and high-fat diet-fed animals (females and males) at 8-16-40 weeks of age. N=44 animals (21 under high-fat vs 23 under chow diet) across 3 timepoints.

Suppl.Fig.1

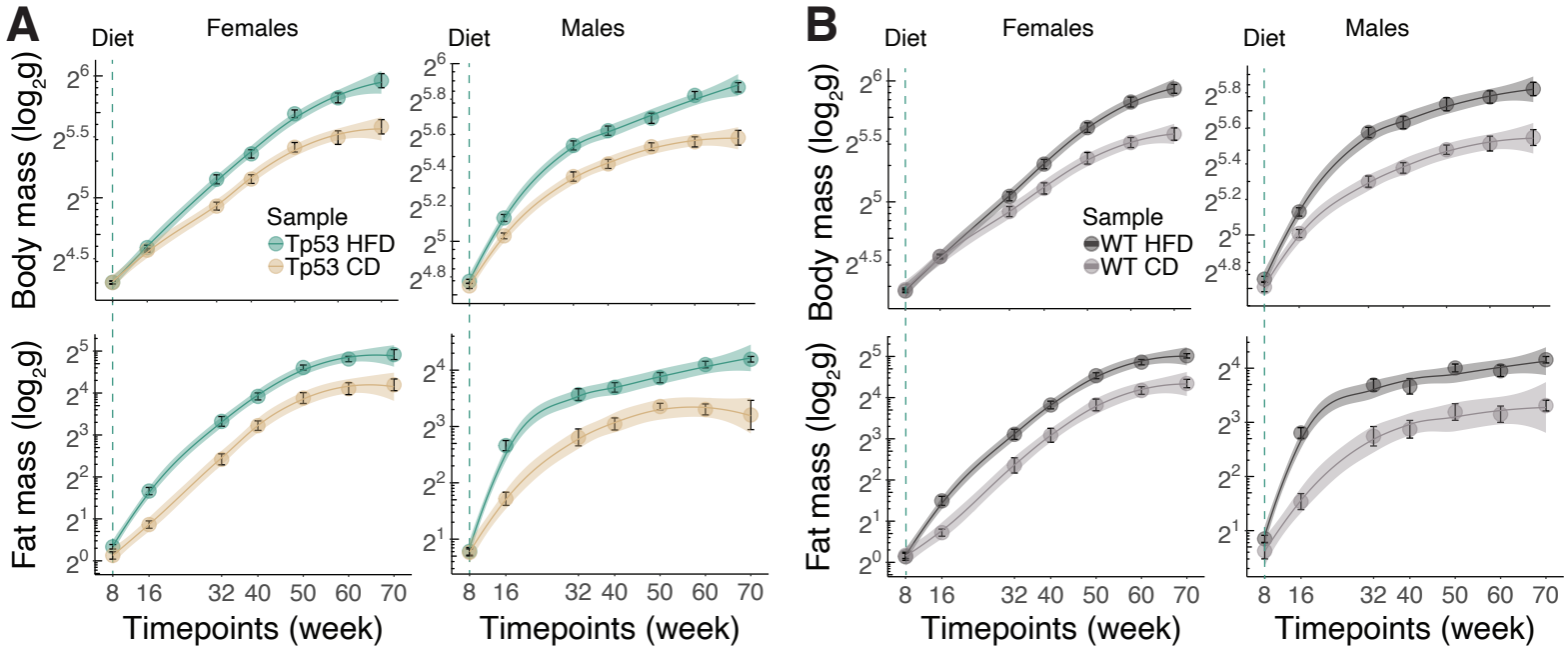
A
Diet
Females
Males
Body mass (log2g)
Fat mass (log2g)
Sample
Tp53 HFD
Tp53 CD
Timepoints (week)
B
WT HFD
WT CD

Supplementary Figure 1. A cohort to study chronic effects of obesity on *Tp53*-dependent cancers across females and males. A) Scatter plots and smoothed conditional means (95% confidence interval, "loess" method) for *body* (top) and *fat* (bottom) mass in *Tp53*$^{+/R270H}$ *females* (left) and *males* (right). N=101 females and 94 males (60 under high-fat and 41 under chow diet) and 94 males (56 under high-fat and 38 under chow diet).. **B)** Scatter plots and smoothed conditional means (95% confidence interval, "loess" method) for *body* (top) and *fat* (bottom) mass in wild-type *females* (left) and *males* (right). N=70 females (40 under high-fat and 30 under chow diet) and 53 males (29 under high-fat and 24 under chow diet).

Fig.2

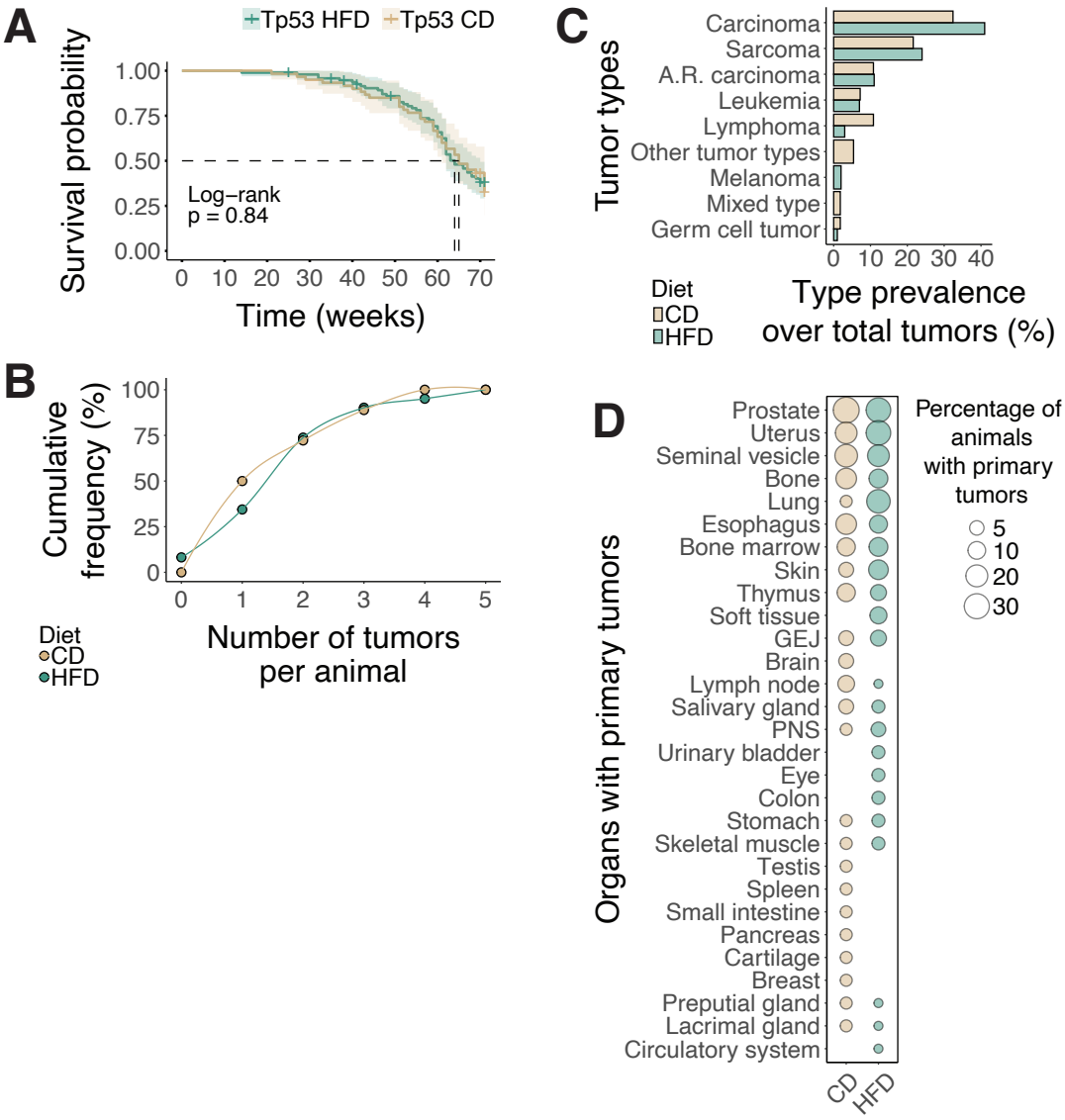
A
Tp53 HFD
Tp53 CD
Survival probability
1.00
0.75
0.50
0.25
0.00
Log−rank
p = 0.84
0 10 20 30 40 50 60 70
Time (weeks)
B
Cumulative frequency (%)
100
75
50
25
0
0 1 2 3 4 5
Number of tumors per animal
Diet
CD
HFD
C
Tumor types
Carcinoma
Sarcoma
A.R. carcinoma
Leukemia
Lymphoma
Other tumor types
Melanoma
Mixed type
Germ cell tumor
0 10 20 30 40
Type prevalence over total tumors (%)
Diet
CD
HFD
D
Organs with primary tumors
Prostate
Uterus
Seminal vesicle
Bone
Lung
Esophagus
Bone marrow
Skin
Thymus
Soft tissue
GEJ
Brain
Lymph node
Salivary gland
PNS
Urinary bladder
Eye
Colon
Stomach
Skeletal muscle
Testis
Spleen
Small intestine
Pancreas
Cartilage
Breast
Preputial gland
Lacrimal gland
Circulatory system
CD
HFD
Percentage of animals with primary tumors
5
10
20
30

Figure 2. HFD does not alter survival, burden, or spectrum in *Tp53*$^{R270H/+}$ mice. A) Kaplan-Meier survival probability by diet for *Tp53*$^{+/R270H}$ animals. Log-rank test, p=0.84. N=155 animals (95 high-fat diet vs 60 chow diet, pooled female and male data). **B)** Cumulative distribution of tumor burden (number of tumors per animal) in *Tp53*$^{+/R270H}$ animals fed with chow- or high-fat diet. N=97 animals (61 high-fat diet vs 36 chow diet, pooled female and male data). **C)** Prevalence of each tumor type over the total number of tumors in chow- or high-fat diet-fed *Tp53*$^{+/R270H}$ animals. N=168 tumors (108 tumors in high-fat diet- vs 60 in chow diet-fed animals, pooled female and male data). **D)** Percentage of *Tp53*$^{+/R270H}$ animals with primary tumors targeting the different organs. N=92 animals (61 high-fat diet vs 36 chow diet, pooled female and male data).

Suppl.Fig.2

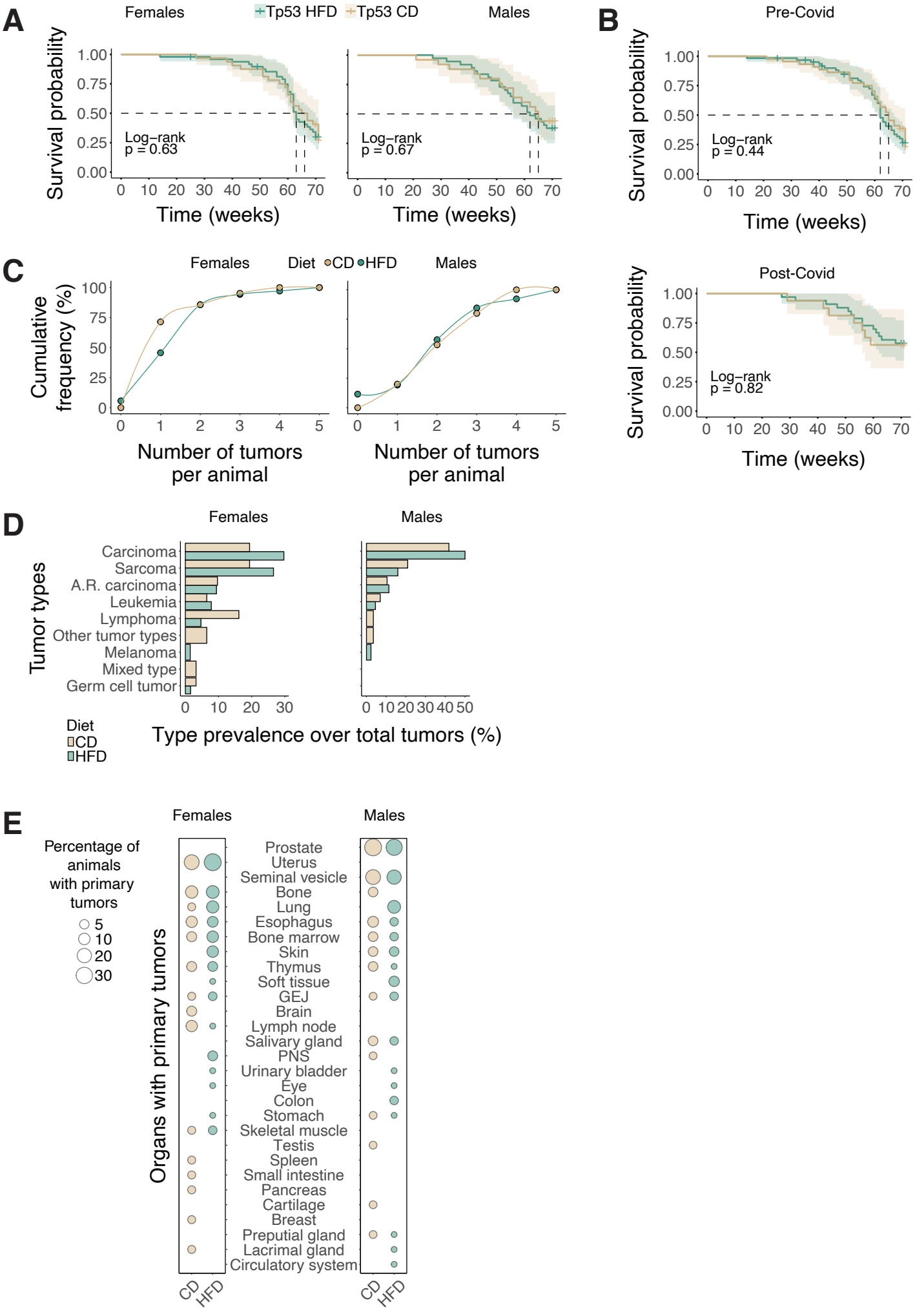
A
Females
Tp53 HFD
Tp53 CD
Males
Survival probability
Log−rank
p = 0.63
Log−rank
p = 0.67
Time (weeks)
B
Pre-Covid
Log−rank
p = 0.44
Post-Covid
Log−rank
p = 0.82
C
Diet
CD
HFD
Cumulative frequency (%)
Number of tumors per animal
D
Tumor types
Carcinoma
Sarcoma
A.R. carcinoma
Leukemia
Lymphoma
Other tumor types
Melanoma
Mixed type
Germ cell tumor
Type prevalence over total tumors (%)
E
Percentage of animals with primary tumors
Organs with primary tumors
Prostate
Uterus
Seminal vesicle
Bone
Lung
Esophagus
Bone marrow
Skin
Thymus
Soft tissue
GEJ
Brain
Lymph node
Salivary gland
PNS
Urinary bladder
Eye
Colon
Stomach
Skeletal muscle
Testis
Spleen
Small intestine
Pancreas
Cartilage
Breast
Preputial gland
Lacrimal gland
Circulatory system

Supplementary Figure 2. HFD does not alter survival, burden, or spectrum in *Tp53*$^{R270H/+}$ female or male mice. A) Kaplan-Meier survival probability by diet for *Tp53*$^{+/R270H}$ *females* (left) or *males* (right). Log-rank test, p=0.64 and p=0.67, respectively. N=81 females (49 high-fat diet vs 32 chow diet) and 74 males (46 high-fat diet vs 28 chow diet). **B)** Kaplan-Meier survival probability by diet for *Tp53*$^{+/R270H}$ animals in the *pre-Covid* (left) or *post-Covid* (right) cohorts. Log-rank test, p=0.44 and p=0.82, respectively. N=106 pre-Covid (62 high-fat vs 44 chow diet) and 49 post-Covid (33 high-fat vs 16 chow diet). **C)** Cumulative distribution of tumor burden (number of tumors per animal) in *Tp53*$^{+/R270H}$ *females* (left) or *males* (right) fed with chow- or high-fat diet. N=56 females (35 high-fat diet vs 21 chow diet) and 41 males (26 high-fat vs 15 chow diet). **D)** Prevalence of each tumor type over the total number of tumors in chow- or high-fat diet-fed *Tp53*$^{+/R270H}$ animals. N=95 tumors in females (64 in high-fat diet vs 31 in chow diet) and 73 in males (44 in high-fat diet vs 29 in chow diet). **E)** Percentage of *Tp53*$^{+/R270H}$ animals with primary tumors targeting the different organs. N=54 females (33 high-fat diet vs 21 chow diet) and 38 males (23 high-fat diet vs 15 chow diet).